ASSESSMENT OF TEMPORAL VARIABILITY FOR AGRICULTURAL LAND BY FRACTAL ANALYSIS OF SATELLITE IMAGERY

F. SALA[1], C. A. POPESCU[2], M. V. HERBEI[2,*]
Banat University of Agricultural Sciences and Veterinary Medicine "King Michael I of Romania" from Timisoara, Timisoara, 300645, Romania
[1]Soil Science and Plant Nutrition; [2]Remote Sensing and GIS
corresponding author: [*]E-mail address: mihaiherbei@usab-tm.ro

Abstract. *The study used fractal analysis and remote sensing technique to analyze and describe the temporal variation of an agricultural area. The satellite images (10 images) were achieved in the Rapid Eye system (RGB - 321, False Color - 532), between 28.03 - 31.10 2017. The study was carried out over a total time interval (T) of 218 days, with several partial intervals between the moments of the satellite images acquisition (t), that varied between 10 and 49 days. The fractal analysis was performed on the binarized images, using the box-counting method. Fractal dimensions (D) were obtained in conditions of statistical accuracy (R^2 for D=0.999). Fractal dimensions had values ranging between D=1.735 (trial 9, data 29.09) and D=1.810 (trial 1, data 28.03). ANOVA test, single factor, highlighted the existence of variance in the experimental data set and statistical accuracy of the data (F>Fcrit, p<<0.001), under conditions of Alpha=0.001. There were identified very high negative correlations between D and T (r=-0.942). The variation of the fractal dimension (D) with respect to T has been accurately described by a polynomial model of degree 2, under conditions of R=0.951, p<<0.001, and by a model of smoothing spline, under conditions of statistical certainty ($\bar{\varepsilon} = 0.001289$). In the framework of PCA analysis, PC1 has explained 87.845% of variance, and PC2 has explained 10.688% of variance. Cluster analysis, based on fractal dimensions (D), led to the grouping of the studied cases, associated with the ten moments of time, according to the Euclidean distances, under statistical accuracy conditions (Coph.corr=0.895). Variants were found to be grouped into two distinct clusters. With a high degree of affinity, variants were associated as follows, 4 with 5 (sample data 28.06, 08.07), subcluster C1, variants 7 with 8 (sample data 19.08, 10.09) and variants 9 with 10 (sample data 29.09, 31.10), subcluster C2, respectively variants 2 with 3 (sample data 15.05, 03.06), subcluster C3. Estimating a moment in time T depending on the values of the fractal dimensions (D) was possible on the basis of a model expressed by a polynomial equation of 3rd degree, under conditions of statistical accuracy R^2=0.947, p=0.00031.*

Keywords: *agricultural land, fractal analysis, fractal dimension, PCA, temporal variability*

INTRODUCTION

The temporal variation of land areas, land cover and agricultural crops has been extensively studied in relation to different natural or anthropogenic factors (HERBEI and SALA, 2015; CUI et al., 2016; YIN et al., 2018; REYES and ELIAS, 2019).

In order to increase the accuracy of work in the momentary or dynamic evaluation of crops or other areas studied, studies have been carried out on the processing and analysis of satellite images and the evaluation of interdependence relations between spectral information and specific indices (UPADHYAY et al., 2012; HERBEI and Sala, 2014; HERBEI et al., 2015a; AL-SADDIK et al., 2019). Studies have also been carried out regarding the analysis and classification of agricultural crops by crop types, vegetation status, vegetation indices, health conditions, stress, production, etc. (HERBEI et al., 2015b; AVOLA et al., 2019; YEOM et al., 2019; KOBAYASHI et al., 2020).

Related to these studies on the temporal spatial variability of agricultural crops (BANIYA et al., 2019; RIO-MENA et al., 2020) several researches are justified and carried out regarding the optimization of some inputs, as production factors influencing the spatial-temporal variation of agricultural crops (SU et al., 2018; XU et al., 2019). Thus, several researches have highlighted the influence of fertilization in crop variability expressed by physiological indices (DATCU and SALA, 2018a), productivity elements (RAWASHDEH and SALA, 2014, 2016; DATCU et al., 2019), productions and quality indices of different crop species (DOBREI et al., 2010; RAWASHDEH and SALA, 2015; DATCU and SALA, 2018b). A series of other production factors, such as biological material, irrigation water, agricultural technique, etc. were analyzed in relation to the temporal and spatial variation of agricultural crops (MALI and SINGH, 2015; CALERA et al., 2017; MASINO et al., 2018).

Also justified and very important are the studies of optimization of inputs in the agricultural production process (BANSOD et al., 2013; SALA et al., 2015; SHAH and WU, 2019). Knowledge of such aspects may explain certain trends in temporal and spatial variation of agricultural areas (WONG and ASSENG, 2006; FILHO et al., 2010; CHEN et al., 2011). The punctual evaluation of these aspects, in relation to the spatial-temporal variation, can explain certain aspects in the dynamics of agricultural crops and productions and can also offer solutions for optimization of inputs (KNAPP and VAN DER HEIJDEN, 2018; MAESTRINI and BASSO, 2018).

Imaging methods for assessing spatial and temporal variability have high efficiency as a result of being adaptable from small surfaces to large areas, at different times frames, allow real-time analysis, but also retrospective analysis (post factum) or predictive analyses, facilitate the creation of models, allow implementation in IT technologies, promote digitization in agriculture, have affordable costs (ALI et al., 2019; KAYAD et al., 2019). In this context, fractal analysis provides a number of study facilities and also high accuracy in assessing fractal geometry in the dynamics of terrestrial or agricultural areas, which recommends it as a method and study tool (EGHBALL et al., 1999; VIDAL-VÁZQUEZ et al., 2012).

This study analyzed and evaluated the temporal variability of an agricultural area through fractal analysis of satellite images.

MATERIAL AND METHODS

The study used fractal analysis to assess and describe the temporal variation of an agricultural area.

The perimeter studied lies within the Western Plain, with the location within SD Timisoara. The studied variation of fractal geometry was captured in satellite images of the agricultural area studied, between 28 March and 31 October 2017. The total study interval (T) was 218 days, with several partial time intervals (t), given by the moments of satellite image collection, and which ranged from 10 to 49 days.

The Rapid Eye satellite system was used to retrieve satellite images (RGB-321, False Color-532). 10 satellite images were taken at set times within the study range.

Fractal analysis was performed on binary images, the source images being obtained from the combination NIR-Red-Green, figure 1. The box-counting method was used for fractal analysis (VOSS, 1985), relations (1), (2), (3), (RASBAND et al., 1997).

$$\text{Mean D} = \sum(D)/\text{GRIDS} \tag{1}$$

$$D = m\left[\frac{\ln(F)}{\ln(\varepsilon)}\right] \tag{2}$$

where: D – fractal dimension; m – slope to regression line, in eq. (3); F – number of new part; ε – scale applied

$$m = \left(n\sum SC - \sum S \sum C\right) / \left(n \sum S^2 - \left(\sum S\right)^2\right) \tag{3}$$

where: m – slope of regression line; S – log of scale or size; C – log of count; n – number of size

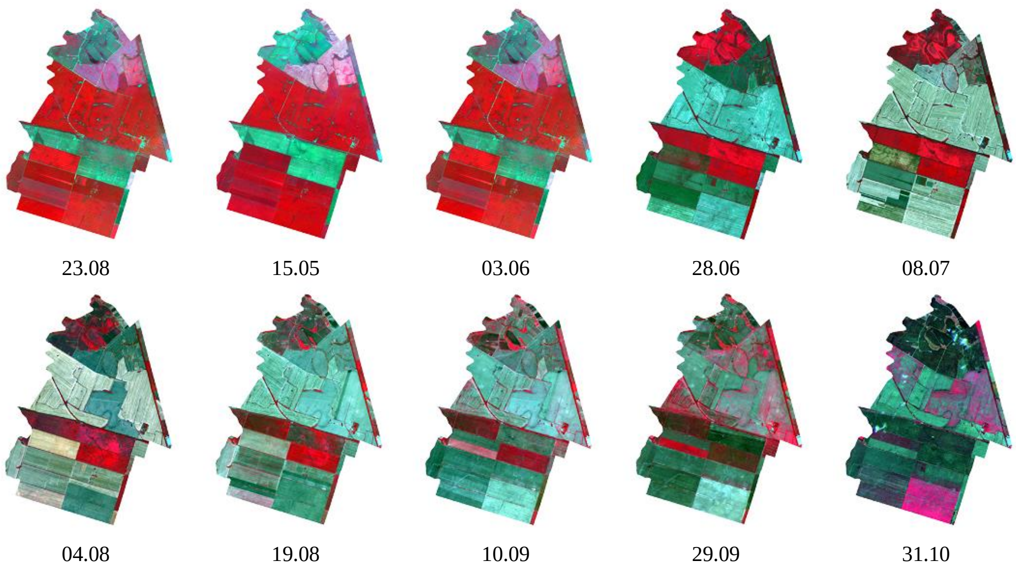

Figure 1. Images in false colors during the study period, SD Timisoara, used in fractal analysis

For the analysis and evaluation of the temporal variability of the agricultural area in the study, the fractal dimension (D) was used in relation to the total time (T) and the partial time (t) at which the study was reported. Also, a comparative analysis was done of the variation in fractional dimensions D with the data communicated by the HERBEI et al. (2018) for indices NDVI (ROUSE et al., 1974), SAVI (HUETE, 1988), PSRI (MERZLYAK et al., 1999), respectively band REG EDGE.

The ANOVA test was used to assess variance and statistical accuracy in the experimental dataset. Correlation analysis, regression, cluster analysis and PCA analysis e used to assess the interdependence of the evaluated parameters (HAMMER et al., 2001). The accuracy of the results was assessed on the basis of specific statistical accuracy coefficients and parameters (r, R^2, p, $\bar{\varepsilon}$, Coph.corr).

RESULTS AND DISCUSSIONS

The images studied were analyzed by the box-counting method for the evaluation of fractal geometry and resulted in fractal dimensions (D). The images showed an equal initial resolution, with a total number of pixels (TP) 846423. At the same time, the binarized images, used in fractal analysis, showed a variable number of foreground pixels (FP), with values ranging between FP=179797 (trial 5) and FP=284800 (trial 3). Fractal dimension values (D) ranged from D=1.735 (trial 9) and D=1.810 (trial 1), Table 1. The ANOVA test confirmed statistical accuracy and the presence of variance in the experimental data set (F>Fcrit, $p<<0.001$), Table 2.

To analyze and describe the temporal variation of the agricultural area studied based on fractal geometry, the level of correlation of fractal dimensions (D) was analyzed with the time factor (T) on which the study was conducted. A very high negative correlation was found between D and T (r=-0.942), and the variation in fractional dimension D in relation to the time factor (T) was described by both a 2nd degree polynomial model , under conditions of R^2=0.951, p<<0.001, as well as a smoothing spline model, under conditions of statistical accuracy ($\bar{\varepsilon} = 0.001289$), relation (4). The values of the smoothing spline model are shown in Table 3, and the graphical distribution of D values in relation to time (T) is presented in figure 2.

Table 1

Experimental data on fractal dimension during the study period and image properties

Trial	Data	Time interval		Fractal dimension		Foreground Pixels	Total Pixels
		t	T	D	R^2 for D		
1	28 03	0	0	1.810	0.999	258804	846423
2	15 05	49	49	1.796	0.999	275359	
3	03 06	19	68	1.783	0.999	284800	
4	28 06	25	93	1.757	0.998	232481	
5	08 07	10	103	1.758	0.999	179797	
6	04 08	27	130	1.749	0.999	218163	
7	19 08	15	145	1.739	0.999	187282	
8	10 09	22	167	1.740	0.999	211138	
9	29 09	19	186	1.735	0.998	210204	
10	31 10	32	218	1.737	0.999	199711	

Table 2

ANOVA test, single factor

Source of Variation	SS	df	MS	F	P-value	F crit
Between Groups	4.33E+11	6	7.22E+10	383.0568	1.37E-47	4.33953
Within Groups	1.19E+10	63	1.89E+08			
Total	4.45E+11	69				

Alpha=0.001

$$\bar{\varepsilon} = \left(\sum_{i=1}^{n} \varepsilon_i \right) / n = \left(\sum_{i=1}^{n} \left| \frac{ys_i - y_i}{y_i} \right| \right) / n \qquad (4)$$

Table 3

Statistical data for the Spline model

Trial	xi	D values and parameters in relation to T			
		y_i	ys_i	ε_i	$I_{i/1}$
1	0	1.81	1.8112	0.000663	1
2	49	1.796	1.7931	0.001617	0.990007
3	68	1.783	1.7807	0.001292	0.98316
4	93	1.757	1.7629	0.003347	0.973333
5	103	1.758	1.7572	0.000455	0.970186
6	130	1.749	1.7463	0.001546	0.964167
7	145	1.739	1.7419	0.001665	0.961738
8	167	1.74	1.7381	0.001093	0.95964
9	186	1.735	1.7363	0.000749	0.958646
10	218	1.737	1.7362	0.000461	0.958591
				$\bar{\varepsilon} = 0.001289$	

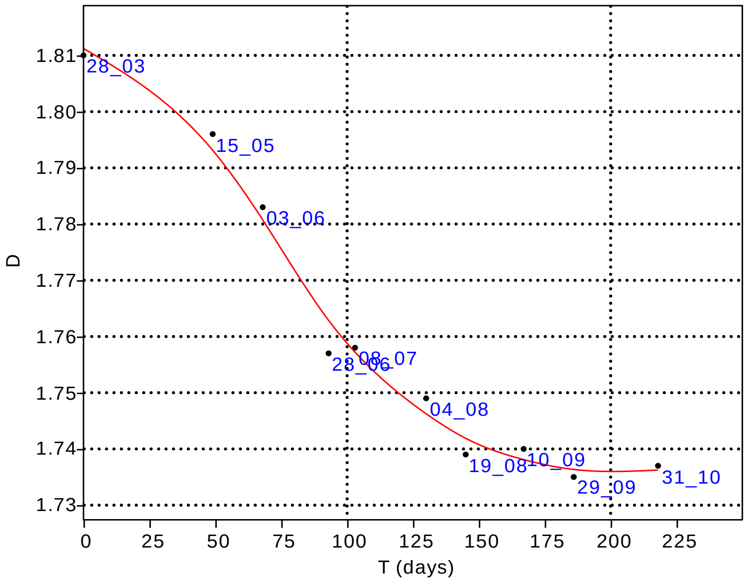

Figure 2. Graphic distribution of values D in relation to T, according to spline model

PCA analyses led to the diagram shown in the figure 3, where PC1 has explained 87.845% of the variance, and PC2 has explained 10.688% of the variance.

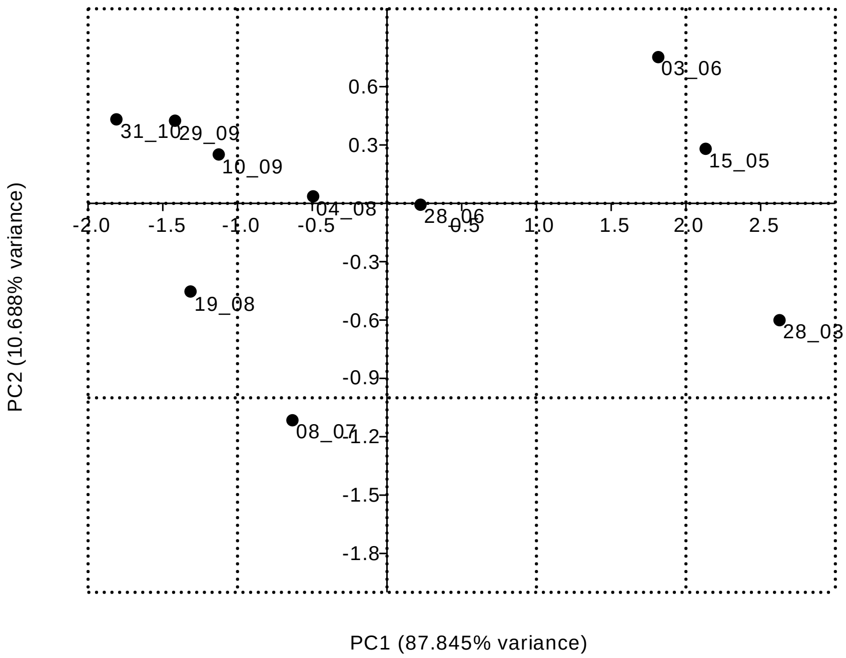

Figure 3. Diagram PCA, distribution of study variants

Cluster analysis led the grouping of variants according to fractal size (D) based on affinity and resulted in the diagram in figure 4, under conditions of high statistical accuracy (Coph.corr.=0.895). Resulted were two distinct clusters with several subclusters each. High affinity was found in variants 4 with 5, then 7 with 8, and respectively 9 with 10.

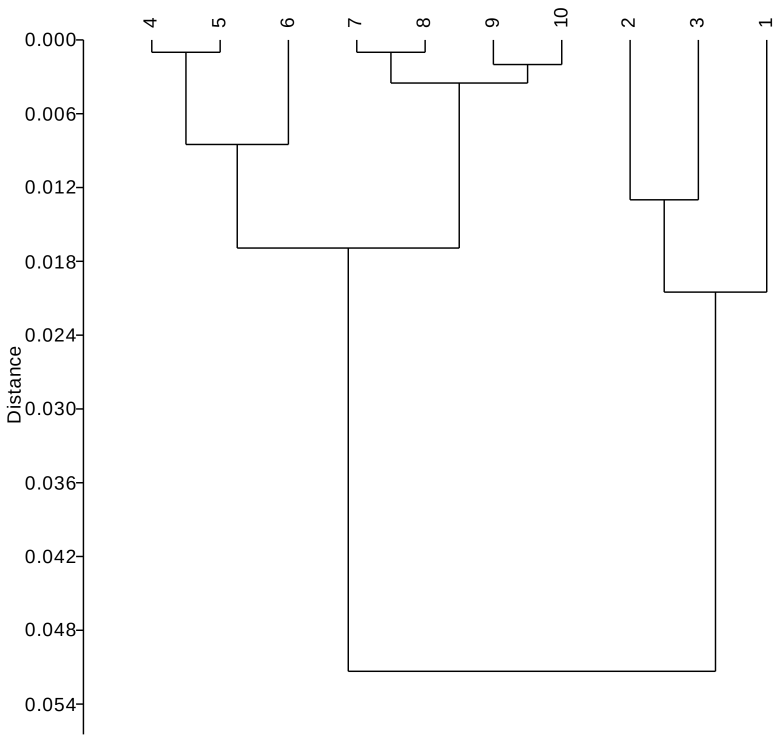

Figure 4. Cluster grouping based on Euclidean distances, in relation to fractal dimensions (D)

Estimation of a time moment (T), characterized specifically by fractal geometry, according to fractal dimension values (D) was possible on the basis of a model in the form of a 3rd degree polynomial equation, relation (5), under conditions of R^2=0.947, p=0.00031, with the graphic distribution in figure 5.

$$T = -1.209E06\,D^3 + 6.444E06\,D^2 - 1.145E07\,D + 6.781E06 \quad (5)$$

The values of the fractal dimensions D recorded a different variation in relation to the time moments (t) when the determinations were made, respectively in relation to the total time interval (T) studied. Thus, a rate of change in D values in relation to time (day) was found as lower at the beginning of the study interval (D/day=0.037) for trial 1 (shown on 15.05, compared to the previous determination, 28.03), and the higher rate of change for trial 5 (D/day=0.176), registered on 08.07 compared to the previous moment 28.06. This change was associated with the harvesting of some crops during that period (wheat), having impact in the manifestation of the fractal geometry on the studied area.

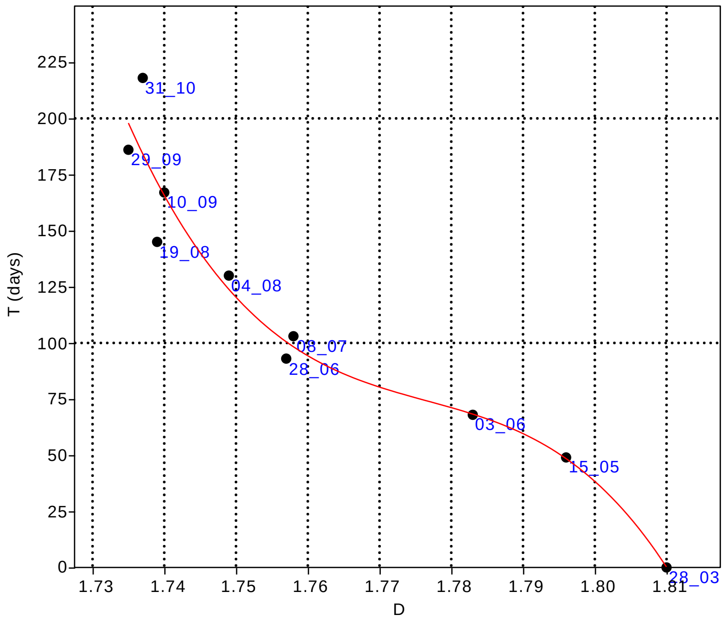

Figure 5. Graphic distribution of values T according to the fractal dimension (D)

Analysis of the distribution of fractal dimensions (D) in relation to vegetation indices NDVI, SAVI, PSRI, respectively with band RED EGDE communicated by HERBEI et al (2018) for that area, revealed the existence of high positive correlations between D and NDVI (r=0.851), between D and SAVI (r=0.848), and medium negative correlations between NDVI and T (r=-0.745), respectively between SAVI and T (r=-0.741). No correlations were recorded between the fractal dimension D and index PSRI, respectively between D and RED EDGE. In relation to the time factor (T), both vegetation indices (NDVI and SAVI), as well as fractal dimension (D) recorded a negative variation. HERBEI et al. (2018) described the variation of the vegetation indices NDVI, SAVI, PSRI and respectively of the spectral band RED EDGE in relation to the time factor using a smoothing spline model, under conditions of statistical accuracy ($\bar{\varepsilon} = 0.064$ for NDVI, $\bar{\varepsilon} = 0.067$ for SAVI, $\bar{\varepsilon} = 0.133$ for PSRI, and respectively $\bar{\varepsilon} = 0.012$ for RED EDGE).

According to HERBEI et al. (2018), the vegetation indices NDVI and SAVI expressed a sinusoidal variation in the vegetation status in the area studied in relation to the time factor, and index PSRI and band RED EDGE captured a variation with variable distribution over the range of time studied.

EGHBAL et al. (2000) used fractal analysis to assess spatial and temporal variability within a soybean crop in relation to mineral and organic fertilization and concluded that fractal analysis, by fractal dimension (D) and covariance were useful in comparative analysis of treatments and in crop management systems.

LA et al. (2009) assessed by fractal analysis the temporal and spatial variability of CO_2 emission in the case of a wheat crop, with a variation in D values between 2 and 2.88, correlated with recorded CO_2 emissions.

Fractal analysis was used to assess the spatial-temporal variation of soil moisture, and the fractal dimension (D) was better than other indicators (nugget/sill ratio) in the description of the temporal variation of soil moisture for the specifics of the studied area, with practical implications in the management of water resources for agriculture (LIAO et al., 2017).

Favorable results in the use of fractal analysis were communicated by WILLIAMS et al. (2019) in a study evaluating the spatial-temporal variation of the complex and dynamic geometry of the dry land alluvial rivers.

Based on the fractal analysis, the present study evaluated the temporal variation of an agricultural area and provided a model of description of this aspect in relation to the time factor (T), under conditions of statistical accuracy.

CONCLUSIONS

The temporal variation of the agricultural area studied, given by agricultural crops and spontaneous vegetation, was highlighted by the analysis of the spectrally captured fractal geometry in the satellite images.

The dynamics of D values in relation to the time factor (T) were described by a 2^{nd} degree polynomial model as well as a spline smoothing model, under conditions of statistical accuracy.

High correlation levels have been identified between fractal dimension D and specific vegetation indices.

ACKNOWLEDGEMENT

The authors thanks to the GEOMATICS Research Laboratory, BUASMV "King Michael I of Romania" from Timisoara, for the facility of the software use for this study.

BIBLIOGRAPHY

AL-SADDIK H., SIMON J.C., COINTAULT F. 2019 – Assessment of the optimal spectral bands for designing a sensor for vineyard disease detection: the case of '*Flavescence dorée*'. Precizion Agriculture, 20: 398-422.

ALI A., MARTELLI R., LUPIA F., BARBANTI L. 2019 – Assessing multiple years' spatial variability of crop yields using satellite vegetation indices. Remote Sensing, 11: 2384.

AVOLA G., DI GENNARO S.F., CANTINI C., RIGGI E., MURATORE F., TORNAMBÈ C., MATESE A. 2019 – Remotely sensed vegetation indices to discriminate field-grown olive cultivars. Remote Sensing, 11: 1242.

BANIYA B., TANG Q., XU X., HAILE G.G., CHHIPI-SHRESTHA G. 2019 – Spatial and temporal variation of drought based on satellite derived vegetation condition index in Nepal from 1982–2015. Sensors 19(2): 430.

BANSOD B.S., PANDEY O.P., RAJESH N.L., DHATTERWAL S. 2013 – Optimisation of agricultural input application to enhance the crop quality and yield quantity in paddy under precision farming. Quality Assurance and Safety of Crops & Foods, 5 (3): 79-185.

CALERA A., CAMPOS I., OSANN A., D'URSO G., MENETI M. 2017 – Remote sensing for crop water management: From ET modelling to services for the end users. Sensors, 17: 1104.

CHEN S.T., HU Z.H., ZHANG Y., SHEN X.S., SHI Y.S. 2011 – Review of the factors influencing the temporal and spatial variability of soil respiration in terrestrial ecosystem. Huan Jing Ke Xue., 32(8): 2184-92.

CUI J., KONG X., LIU Y., WANG S. 2016 – Spatio-temporal variation of agricultural land consolidation in China: case study of Huangshi, Hubei Province. Journal of Maps, 12(sup1): 493-497.

DATCU, A.-D., SALA, F. 2018a – Studies regarding the influence of nitrogen fertilizing dose on some ecophysiological parameters for *Triticum aestivum.* Research Journal of Agricultural Science, 50(4): 105-110.

DATCU, A.-D., SALA, F. 2018b – Nitrogen fertilization effect on aboveground biomass production in *Triticum aestivum*. Research Journal of Agricultural Science, 50(4): 99-104.

DATCU A.-D., IANOVICI N., ALEXA E., SALA F. 2019 – Nitrogen fertilization effects on some gravimetric parameters for wheat. AgroLife Scientific Journal, 8(1): 87-92.

DOBREI A., POIANA M.A., SALA F., GHITA A., GERGEN I. 2010 – Changes in the chromatic properties of red vines from *Vitis vinifera* L. cv. Merlot and Pinot Noir during the course of aging in bottle. Journal of Food, Agriculture & Environment, 8(2): 20-24.

EGHBALL B., HERGERT G.W., LESOING G.W., FERGUSON R.B. 1999 – Fractal analysis of spatial and temporal variability. Geoderma, 88(3-4): 349-362.

EGHBALL B., HERGERT G.W., LESOING G.W., FERGUSON R.B. 2000 – Fractal analysis of spatial and temporal variability. Developments in Soil Science, 27: 259-272.

FILHO O.G., VIEIRA S.R., CHIBA M.K., NAGUMO C.H., DECHEN S.A.C. 2010 – Spatial and temporal variability of crop yield and some Rhodic Hapludox properties under no-tillage. Revista Braileira de Ciência do Solo, 34(1): 1-14.

HAMMER Ø., HARPER D.A.T., RYAN P.D. 2001 – PAST: paleontological statistics software package for education and data analysis. Palaeontologia Electronica, 4(1): 1-9.

HERBEI M., SALA F. 2014 – Using GIS technology in processing and analyzing satellite images–case study Cheile Nerei Beusnița National Park, Romania. Journal of Horticulture, Forestry and Biotechnology, 18(4): 113-119.

HERBEI M.V., SALA F. 2015 – Use landsat image to evaluate vegetation stage in sunflower crops. AgroLife Scientific Journal, 4(1): 79-86.

HERBEI M., SALA F., BOLDEA M. 2015a – Relation of Normalized Difference Vegetation Index with some spectral bands of satellite images. AIP Conference Proceedings, 1648:670003-1 – 670003-4.

HERBEI M., SALA F., BOLDEA M. 2015b – Using mathematical algorithms for classification of Landsat 8 satellite images. AIP Conference Proceedings, 1648: 670004-1 – 670004-4.

HERBEI M.V., POPESCU C.A., HERBEI R.C., RUJESCU C., NICOLIN L.A., SALA F. 2018 – Imagistic analysis and imaging track of a mixed farm based on satellite images. Peoceedings of the International Conference on Life Sciences, 506-515.

HUETE A.R. 1988 – A soil-adjusted vegetation index (SAVI). Remote Sensing of Environment, 25: 295–309

KAYAD A., SOZZI M., GATTO S., MARINELLO F., PIROTTI F. 2019 – Monitoring within-field variability of corn yield using Sentinel-2 and Machine Learning Techniques. Remote Sensing, 11: 2873.

KNAPP S., VAN DER HEIJDEN M.G.A. 2018 – A global meta-analysis of yield stability in organic and conservation agriculture. Nature Communications, 9: 3632.

KOBAYASHI N., TANI H., WANG X., SONOBE R. 2020 – Crop classification using spectral indices derived from Sentinel-2A imagery. Journal of Information and Telecommunication, 4(1): 67-90.

LA N., PANOSSO A.R., PEREIRA G.T., GONZALEZ A.P., MIRANDA J.G.V. 2009 – Fractal dimension and anisotropy of soil CO2 emission in an agricultural field during fallow. International Agrophysics, 23(4): 353-358.

LIAO K., LAI X., ZHOU Z., ZHU Q. 2017 – Applying fractal analysis to detect spatio-temporal variability of soil moisture content on two contrasting land use hillslopes. Catena, 157: 163-172.

MESTRINI B., BASSO B. 2018. Drivers of within-field spatial and temporal variability of crop yield across the US Midwest. Scientific Reports, 8: 14833.

MALI S.S., SINGH D.K. 2015 – Mapping spatial variability in crop evapotranspiration and defining spatial resolution units for crop water footprint assessment at river basin scale. The Ecoscan, 9(1&2): 75-79.

MASINO A., RUGERONI P., BORRÁS L., ROTUNDO J.L., 2018 – Spatial and temporal plant-to-plant variability effects on soybean yield. European Journal of Agronomy, 98: 14-24.

MERZLYAK M.N., GITELSON A.A., CHIVKUNOVA O.B., RAKITIN V.Y. 1999 – Non-destructive optical detection of pigment changes during leaf senescence and fruit ripening. Physiologia Plantarum, 106(1): 135-141.

RAWASHDEH H.M., SALA F. 2014 – Foliar application of boron on some yield components and grain yield of wheat. Academic Research Journal of Agricultural Science and Research, 2(7): 97-

101.
RAWASHDEH H., SALA F. 2015 – Effect of some micronutrients on growth and yield of wheat and its leaves and grain content of iron and boron. Bulletin USAMV series Agriculture, 72(2): 503-508.
RAWASHDEH H., SALA F. 2016 – The effect of iron and boron foliar fertilization on yield and yield components of wheat. Romanian Agricultural Research, 33: 241-249.
REYES J.J., ELIAS E. 2019 – Spatio-temporal variation of crop loss in the United States from 2001 to 2016. Environmental Research Letters, 14(7): 074017.
RIO-MENA T., WILLEMEN L., VRIELING A., NELSON A. 2020 – Understanding intra-annual dynamics of ecosystem services using satellite image time series. Remote Sensing, 12(4): 710.
ROUSE J.W., HAAS R.H., SCHELL J.A., DEERING D.W. 1974 – Monitoring vegetation systems in the great plains with ERTS. In: Proceedings third Earth resources technology satellite-1 symposium, Greenbelt, NASA SP– 351(1): 3010–3017.
SALA F., BOLDEA M., RAWASHDEH H., NEMET I. 2015 – Mathematical model for determining the optimal doses of mineral fertilizers for wheat crops. Pakistan Journal of Agricultural Sciences, 52(3): 609-617.
SHAH F., WU W. 2019 – Soil and crop management strategies to ensure higher crop productivity within sustainable environments. Sustainability, 11: 1485.
SU B., ZHAO G., DONG C. 2018 – Spatiotemporal variability of soil nutrients and the responses of growth during growth stages of winter wheat in northern China. PLoS ONE, 13(12): e0203509.
UPADHYAY P., KUMAR A., ROY P.S., GHOSH S.K., GILBERT I. 2012 – Effect on specific crop mapping using WorldView-2 multispectral add-on bands: soft classification approach. Journal of Applied Remote Sensing, 6: 063524-1 - 063524-13.
VIDAL-VÁZQUEZ E., PAZ-FERREIRO J., VIEIRA S., TOPP G., MIRANDA J., PAZ G.A. 2012 – Fractal description of the spatial and temporal variability of soil water content across an agricultural field. Soil Science, 177(2): 131-138.
WILLIAMS Z.C., PELLETIER J.D., MEIXNER T. 2019 – Self-affine fractal spatial and temporal variability of the San Pedro River, Southern Arizona. JGR Earth Surface, 124(6): 1540-1558.
WONG M.T.F., ASSENG S. 2006 – Determining the causes of spatial and temporal variability of wheat yields at sub-field scale using a new method of upscaling a crop model. Plant and Soil, 283: 203-215.
XU X., HE P., PAMPOLINO M.F., QIU S., ZHAO S., ZHOU W. 2019 – Spatial variation of yield response and fertilizer requirements on regional scale for irrigated rice in China. Scientific Reports, 9: 3589.
YEOM J., JUNG J., CHANG A., ASHAPURE A., MAEDA M., MAEDA A., LANDIVAR J. 2019 – Comparison of vegetation indices derived from UAV data for differentiation of tillage effects in agriculture. Remote Sensing, 11(13): 1548.
YIN H., PRISHCHEPOV A.V., KUEMMERLE T., BLEYHL B., BUCHNER J., RADELOFF V.C. 2018 – Mapping agricultural land abandonment from spatial and temporal segmentation of Landsat time series. Remote Sensing of Environment, 210: 12-24.